Available online at www.sciencedirect.com
SCIENCE DIRECT
Journal of Catalysis 237 (2006) 393–404
JOURNAL OF CATALYSIS
www.elsevier.com/locate/jcat

In situ FTIR study of photocatalytic NO reaction on photocatalysts under UV irradiation

Jeffrey C.S. Wu *, Yu-Ting Cheng

Department of Chemical Engineering, National Taiwan University, Taipei, Taiwan 10617, ROC

Received 7 September 2005; revised 18 November 2005; accepted 21 November 2005

Abstract

The photocatalytic reaction of nitric oxide (NO) on TiO_2 and transition metal-loaded M (Cu, V, and Cr)/TiO_2 catalysts was studied using in situ FTIR spectroscopy under UV irradiation. TiO_2 and M/TiO_2 catalysts were prepared by the sol–gel method via controlled hydrolysis of titanium (IV) butoxide. Copper, vanadium, or chromium was loaded onto TiO_2 during the sol–gel procedure. After treatment at 500 °C under air flow, a large amount of surface peroxo species and OH groups were detected on the TiO_2 and M/TiO_2 catalysts. Nitric oxide was adsorbed on TiO_2 and M/TiO_2 in the form of bidentate nitrites and nitrates by reacting with OH groups, peroxo, or M=O species. In addition, NO can also be adsorbed on M^{n+} in the form of nitrosyls. Under UV irradiation, bidentate nitrite was oxidized to either monodentate or bidentate nitrate. Such oxidation was suggested to be induced by superoxo species generated by oxidizing peroxo species via photogenerated holes. The existence of nitrosyls deferred the oxidation of nitrites to nitrates due to the prior oxidation of nitrosyls by superoxo. The XRD and UV–vis spectra showed that the structures and the abilities of absorbing UV light of all catalysts were not influenced by the photocatalytic NO reaction. Possible mechanisms were proposed for the photocatalytic NO oxidation on TiO_2 and M/TiO_2 based on the intermediates found from the in situ FTIR study.

Keywords: Photocatalysis; Nitric oxide; Titania; In situ FTIR; Cu; V; Cr

1. Introduction

Titania (TiO_2) has attracted much attention in photocatalysis for more than 30 years. Scientists and engineers have devoted themselves to studying and developing applications of TiO_2. Unlike traditional catalysts that drive chemical reactions by thermal energy, semiconducting photocatalysts induce chemical reactions by inexhaustible sunlight. Thus, photocatalysts exhibit the potential for "green Earth" applications.

Nitric oxide (NO) is a major air pollutant generated from either the reaction of N_2 and O_2 or the oxidation of amine compounds in gasoline at high-temperature conditions. Internal combustion engines and boilers are two primary NO sources. The dissolution of NO in raindrops at the atmosphere and the reduction of NO in the ozonosphere result in acid rain and the destruction of the ozone layer, respectively. Nitric oxide can also be oxidized to NO_2 in the presence of peroxide radical, initiating the photochemical cycle to form smog. Even a relatively small quantity of NO can produce large amounts of air pollutants. Thus, NO removal is an important issue in environmental protection.

Many technologies have been developed to remedy NO pollutants, including catalytic oxidation and selective catalytic reduction. Mechanisms of these thermal NO reactions (e.g., oxidation, reduction, decomposition) have been extensively studied. Recently, a photocatalyst, TiO_2, has been used to decompose NO because of its advantage in using photoenergy [1,2]. Unlike thermal NO reactions, the mechanism of photocatalytic NO reaction under UV irradiation requires further investigation to improve the photoefficiency of the photocatalyst.

In general, a photocatalytic reaction usually takes longer (i.e., hours or days) than a thermal reaction, and thus it is possible to observe the changes of intermediates during a photocatalytic NO reaction [3]. In the present work we applied highly sensitive spectral reflectance technique to study a photocatalytic NO reaction on the TiO_2 surface via in situ Fourier

* Corresponding author. Fax: +886 236323040.
E-mail address: cswu@ntu.edu.tw (J.C.S. Wu).

0021-9517/$ – see front matter
doi:10.1016/j.jcat.2005.11.023

transform infrared (FTIR) spectroscopy in time sequence. Transition metal-loaded TiO_2 photocatalysts were also studied, to elucidate the metal effects. The focus was on the intermediates and products generated on the surface by photoexcited TiO_2. Possible mechanisms of the photocatalytic reaction were also explored.

2. Experimental

2.1. Preparation of photocatalysts

The catalysts were prepared via the controlled hydrolysis of titanium(IV) butoxide, as shown in Fig. 1. Slow esterification by the reaction of *n*-butanol and acetic acid provided the water source for hydrolysis [4]. These reagents were added with stoichiometric molar ratio (1:4:4) in a conical flask in the following order: titanium(IV) butoxide (21 ml), *n*-butanol (22 ml), and acetic acid (14 ml). The conical flask was sealed and placed on a magnetic stirrer. Hydrolysis of the titanium butoxide was completed by stirring for 8 h. All processes mentioned were performed in a glove box under the condition of relative humidity <40%. TiO_2 particles loaded with transition metals Cu, V, and Cr were prepared by a similar process. The precursors of the transition metals (copper acetate, vanadyl acetylacetonate, and chromium nitrate) were added to the solution after hydrolyzation for 3 h, after which the solution was continuously stirred for another 5 h. The hydrolyzed solution was dried at 150 °C for 3 h and calcined at 500 °C for 0.5 h. The calcined catalyst was pulverized to powder in an agate mortar. Photocatalysts prepared for this study were assigned as TiO_2, 2 wt% Cu/TiO_2, 1.9 wt% V/TiO_2, and 0.65 wt% Cr/TiO_2. The percentages of metal loadings were the optimal values to give the highest photoactivities in the previous study [4,5]. The weight percentages were calculated from the amounts of metal precursors used in preparation. The crystalline phase and light absorption of catalysts were characterized by X-ray diffraction (XRD) and ultraviolet–visible light (UV–vis) spectroscopy, respectively.

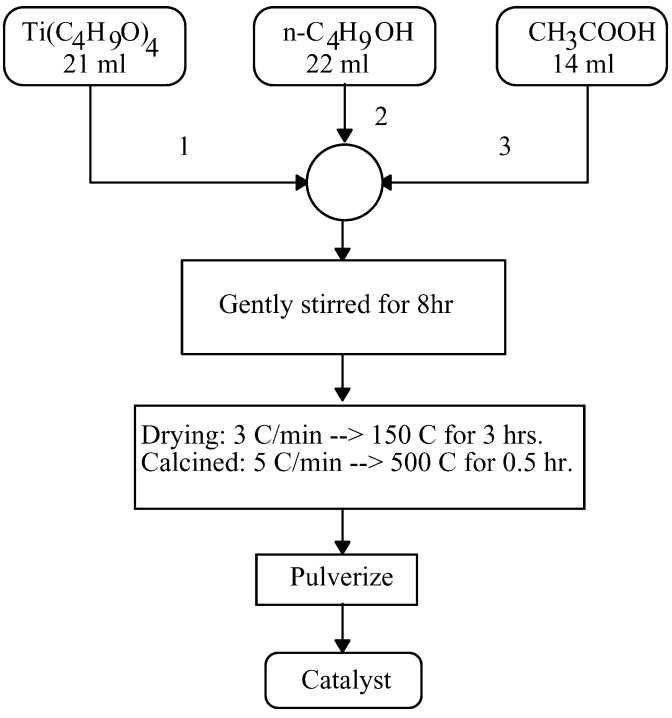

Fig. 1. Procedure of synthesizing pure TiO_2 powders.

2.2. In situ FTIR

The photoreaction of NO was studied by diffuse reflectance infrared Fourier transform (DRIFT) spectroscopy under UV irradiation. Zero-grade air, high-purity He, and 50 ppm of NO (in N_2) mixture can be fed into the reaction system. A three-way ball valve is used to switch either air or He. Gas flow rate and pressure were adjusted by needle valves in the system. To reduce water interference, air and He were passed through a moisture-adsorbing material before entering the photoreactor. Furthermore, all gas (air, He, and NO mixture) was passed through a cold trap (−75 to −95 °C) to remove trace water. A clear IR signal was obtained using this dehumidification apparatus.

A high-temperature chamber (HVC; Harrick HVC-DRP-1) made of 316 stainless steel was used as the photoreactor in this study. The HVC dome contained three windows, including two KBr windows transparent to both IR and UV light for IR transmittance and a quartz window transparent in the UV range but only partly transparent in the IR range for UV irradiation. The HVC was equipped with two gas ports, two coolant ports, and one vacuum port. A K-type thermocouple and an electric heater were connected on the sample cup. The photoreactor was located inside the compartment of the FTIR instrument. Pressure and gas flow rate were measured by a pressure transducer and a bubble flow meter, respectively. A vacuum pump provided suction force to tightly compact the catalyst powder.

A temperature controller directly connected to the thermocouple and heater of the HVC provided accurate temperature control (±1 °C). A mesh was put in the sample cup, which could be filled with catalyst powder using an overflow tray, to prevent the sample powder from being blown out. Gas was introduced from one gas port, flowed through the reactor, and exited from another gas port. The HVC was designed for operation up to 600 °C, but operation at temperatures above 100 °C required water-cooling via the coolant ports connected to a water chiller. The UV light source (EXFO; OmniCure 1000) was supplied by a 100-W Hg lamp with filter (365 nm only). The UV light was transmitted to the quartz window of the HVC by an optical cable.

A catalyst sample of 140–170 mg was pretreated inside the photoreactor under air flow and UV irradiation at 500 °C to remove residual hydrocarbons. Fig. 2 shows the IR spectra of TiO_2 catalyst in air flow at different temperatures. Residual hydrocarbons (1200–1800 cm^{-1}) were effectively removed at 500 °C. The absorption bands at 2358 and 2343 cm^{-1} represented the asymmetric stretching of CO_2 (g) in atmosphere. The catalyst was cooled to 25 °C with a He purge. (Note that the HVC can be accurately controlled at 25 °C by circulating chilled water instead of a temperature controller.) Before the

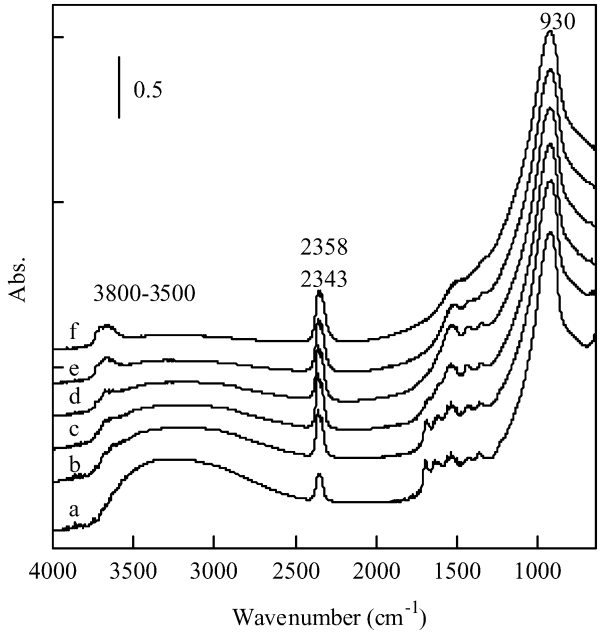

Fig. 2. The IR spectra of TiO_2 pretreated in air at (a) 25 °C, (b) 110 °C, (c) 200 °C, (d) 300 °C, (e) 400 °C, (f) 500 °C.

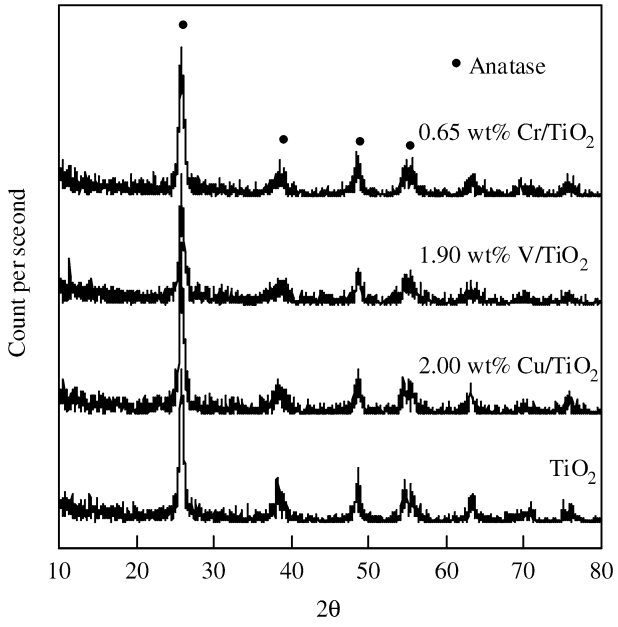

Fig. 3. XRD of the catalysts.

adsorption of NO, an IR spectrum of each catalyst after 500 °C pretreatment was taken as a background reference in He atmosphere at 25 °C. The spectrum of photocatalytic NO reaction of each catalyst was subtracted from its own background. The adsorption of NO on the pretreated catalysts was carried out at 25 °C for 30 min after additional He purging for 5 min. An IR spectrum was obtained without UV light and marked "UV off" in the spectrum; then a photoreaction was performed under UV irradiation in a closed system for 5 h, and the IR spectra were obtained in time sequence. All spectra were recorded during the UV-off period. The IR scanning range was 4000–650 cm^{-1} with 4 cm^{-1} resolution using a mercury-cadmium-telluride detector in a Nexus 470 IR spectrometer (Thermo Nicolet). Each IR spectrum was obtained by 64 scans.

3. Results

Fig. 3 shows the XRD patterns of sol–gel derived catalysts, indicating that catalysts were all anatase-phase crystalline. Transition metals Cu, V, and Cr were well dispersed on TiO_2; no other discernible peaks were found relating to transition metal oxides. The crystal sizes of TiO_2, 2 wt% Cu/TiO_2, 1.9 wt% V/TiO_2, and 0.65 wt% Cr/TiO_2 were 17, 17, 19, and 11 nm, respectively, estimated by Scherrer's equation. Thermal pretreatment and photoreaction procedures caused no significant changes in crystalline size or phase. Fig. 4 shows the UV–vis diffuse reflectance spectra of the catalysts. Each spectrum demonstrated absorption in the region of UV light (<380 nm). Compared with pure TiO_2 catalysts, M (Cu, V, Cr)/TiO_2 exhibited noticeable red shifts of the absorption shoulders into the visible light region, indicating the capability of visible light (420–600 nm) absorption [5].

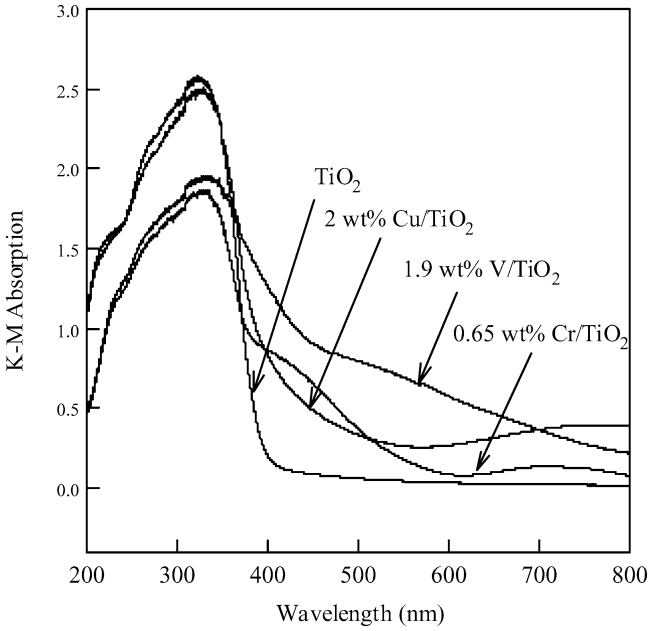

Fig. 4. UV–vis diffusive reflective spectra of the catalysts.

3.1. NO adsorption on TiO_2

Fig. 5 shows the spectra of NO adsorbed on TiO_2 catalyst. In the region of 2300–650 cm^{-1}, several absorption bands were formed on contact of TiO_2 with gaseous NO at 25 °C. A strong absorption band at 1620 cm^{-1} developed progressively with time. In the first 5 min (Fig. 5), a prominent peak at 1576 cm^{-1} and a weak absorption band at 1192 cm^{-1} were observed, and no other discernible peaks were found. As time passed, the intensity of the signal peaked at 1576 cm^{-1} was almost the same as it was at 5 min. Absorption bands at the 1668–1620 cm^{-1} shoulder and at 1540, 1525, 1508, and 1192 cm^{-1} developed progressively, and two weak bands at 2239 and 1458 cm^{-1}

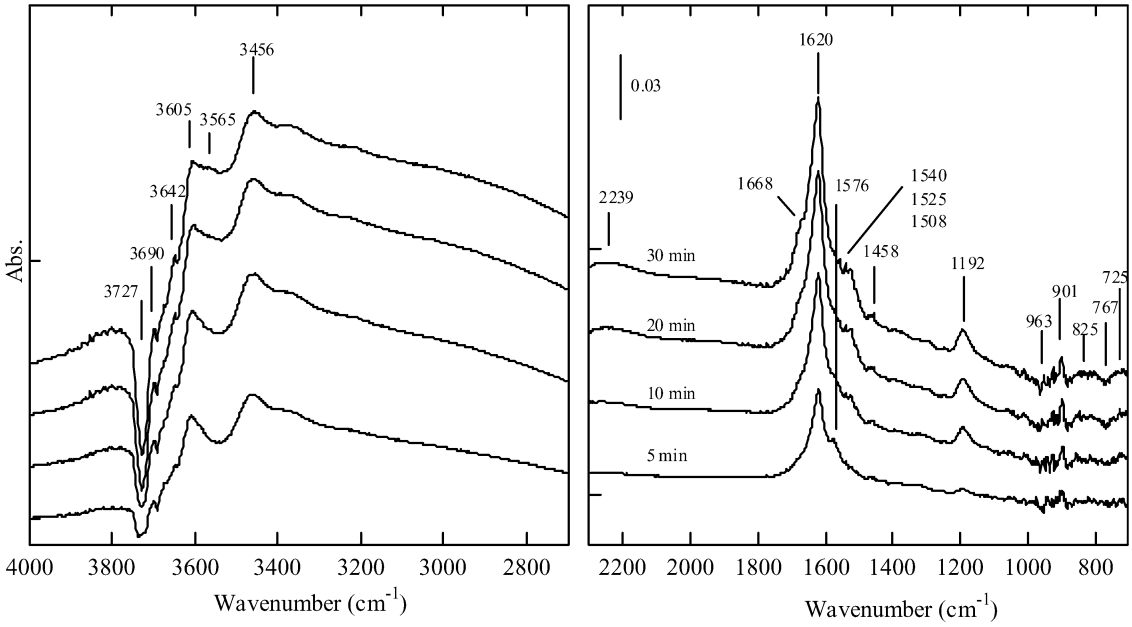

Fig. 5. IR spectra of NO adsorption on TiO_2.

also appeared in the spectra. Two negative bands at 963 and 767 cm^{-1}, a sharp peak at 901 cm^{-1}, and two weak, broad absorption bands at around 825 and 725 cm^{-1} were observed in the region of <1000 cm^{-1}.

In the high-frequency region (4000–2700 cm^{-1}), a strong broad band at 2700–3900 cm^{-1} with its maximum at 3605 and 3456 cm^{-1} was observed in the first 5 min and gradually increased over time. An obvious decrease at 3727 cm^{-1} and two weak decreasing bands at 3690 and 3642 cm^{-1} were observed in the spectrum at 5 min (Fig. 5). As time passed, a sharp decrease at 3727 cm^{-1} and a weak absorption band at 3565 cm^{-1} appeared, while the intensities of peaks at 3690 and 3642 cm^{-1} remained almost unchanged.

Table 1 summaries the assignment of all absorption bands on the TiO_2 catalyst. A strong absorption band at 1620 cm^{-1} was assigned to adsorbed, undissociated H_2O [6,7]. However, this band might be also attributed to the δ (HOH) of OH groups interacting with nitrates. The peak at 1576 cm^{-1} was assigned to bidentate nitrate according to previously published results [6,8,9]. In addition, the peak at 1458 cm^{-1} was assigned to bidentate nitrate; however, its intensity was very weak because it was in almost a symmetric stretching mode [8]. The absorption bands at 1540, 1525, and 1508 cm^{-1} were assigned to monodentate nitrate [6,8,9]. The signal peak at 1192 cm^{-1} can be assigned to nitrite, possibly in the bidentate state [10,11]. Ramis et al. [8] reported that the intensities of 1545 and 1190 cm^{-1} were originally very low but grew later. These findings are consistent with our results.

As for the band of 1668–1620 cm^{-1}, it can be attributed to δ (HOH) of excess H_2O or OH groups interacting with monodentate or bidentate nitrates. Kantcheva et al. [9] noted that monodentate nitrate possibly coupled with adsorbed H_2O and caused bands at 1620 and 1630 cm^{-1}; however, Hadjiivanov and Knözinger [12] assigned the 1600–1650 cm^{-1} band to nitrates, not adsorbed H_2O. The peak at 1620 cm^{-1} is adsorbed

Table 1
Assignments of the FT-IR bands observed upon adsorption of NO on TiO_2 followed by UV irradiation

Wavenumbers (cm^{-1})	Assignment	References
901–680	Surface peroxo, ν(TiOO–)	[14,17,18]
1000–900	$\nu(Ti(O_2))$	[14–16]
1060–1003	Nitrate, possibly in bidentate state, $\nu(NO_3)$	[10,11]
1192	Bidentate nitrite, $\nu(NO_2)$	[10,11]
1253–1241	Bidentate nitrate, $\nu(NO_3)$	[8,10]
1291–1288	Monodentate nitrate, $\nu(NO_3)$	[6,8,9,20]
1458	Almost symmetric stretching mode of bidentate nitrate, $\nu(NO_3)$	[8]
1540–1506	Monodentate nitrate, $\nu(NO_3)$	[6,8,9]
1605–1604, 1586–1576	Bidentate nitrate, $\nu(NO_3)$	[6,8,9]
1620	Adsorbed, undissociated water, $\delta(H_2O)$	[6,7]
1668–1620	δ(HOH) of H_2O or OH groups interacting with monodentate or bidentate nitrate	[9]
1698	Contaminants on the TiO_2 surface	–
2239–2236	May be $\nu(N_2O)$	[8,12,13]
<3400, broad	Undissociated $\nu(H_2O)$	–
3456	Isolated $\nu(H_2O)$	–
3565	ν(OH) of NO–H	[6,20]
3700–3550	H-bonded OH groups	[2]
3750–3700	Surface free OH groups	[2]
3900–2500, extended	Delocalized protons	[19]

H_2O, but may be overlapped with the band at 1668–1620 cm^{-1}, which is attributed to HOH coupled with nitrates. Some investigators assigned the band of 2239 cm^{-1} to N_2O [8,12,13] and found that it increased at the beginning of NO adsorption and then decreased over time (in h).

In the region of 1000–650 cm^{-1}, although the absorption bands were affiliated with the O–O stretching mode of surface peroxo species, it was difficult to elucidate every absorption band, because many different structures caused similar absorption bands in this region, and different absorption ranges were

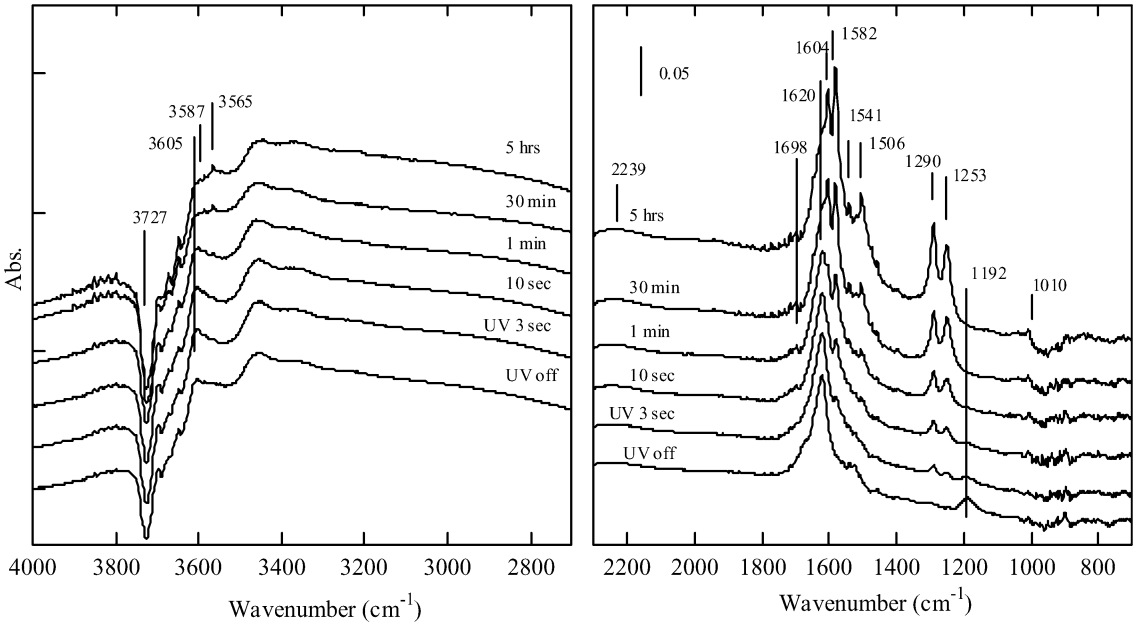

Fig. 6. IR spectra of photocatalytic reaction of NO on TiO_2 under UV irradiation.

sometimes assigned to the same peroxo species. For example, titanium dioxygen adducts were reported in the O–O stretching band for peroxide, $Ti(O_2)$, located at 950–890 cm^{-1} [14,15] or 932–800 cm^{-1} [15,16], with that for another kind of bridged peroxide, TiOOTi or TiOOH (hydroperoxo), located at 770–700 cm^{-1} [9,11] or 790–840 cm^{-1} [17]. We suggested assigning the absorption bands formed on adsorption of NO to $Ti(O_2)$ at 1000–900 cm^{-1} [14–16]. In addition, different structures of surface peroxides with O–O bonds were suggested to be in the form of TiOO– at absorption bands 901, 870–770, 767, and 750–680 cm^{-1} [14,17,18].

In high-frequency region, five kinds of ν(OH) were classified: extremely extended bands at 3900–2500 cm^{-1}, 3750–3700 cm^{-1}, 3700–3550 cm^{-1}, and 3500–3400 cm^{-1} and a broad band at below 3400 cm^{-1}. These were assigned to delocalized protons [19], surface free OH groups [2], H-bonded OH groups [2], isolated H_2O, and undissociated H_2O, respectively. Some investigators assigned peaks at 3750–3550 cm^{-1} to "isolated OH groups" [6,9,19]; however, we assigned them to "splitting OH groups," which were not in the form of H_2O [2]. Under water-poor condition, like our reaction system, the peak at 3456 cm^{-1} became clearly observable and was not as broad as the band at below 3400 cm^{-1}. Thus we regarded the former (3456 cm^{-1}) as a ν(OH) mode of isolated H_2O and the latter (below 3400 cm^{-1}) as undissociated H_2O. The band of 3565 cm^{-1} that increased over time was assigned to ν(OH) of NO–H [6,20].

3.2. Photocatalytic NO reaction on TiO_2

Fig. 6 shows the spectra of NO adsorbed on TiO_2 during UV irradiation in time sequence. The spectrum of "UV off" is the same as that of "30 min" in Fig. 5, at which NO adsorption reached equilibrium close to 30 min after introducing NO in the absence of UV light. In the high-frequency region there was no change on 1-min of UV irradiation. In contrast, only 3-s of UV irradiation caused significant changes in the low-frequency region of 1700–650 cm^{-1}. A peak at 1192 cm^{-1} decreased, and new absorption bands at 1582, 1290, and 1253 cm^{-1} appeared. Further UV irradiation resulted in increasing absorption bands at 1698, 1604, 1582, 1290, and 1253 cm^{-1} and a disappearing peak at 1192 cm^{-1}. No intensity changes were observed at the peaks of 1620 and 1540–1506 cm^{-1}. Only negligible changes of spectra were observed for the surface peroxo region (1000–650 cm^{-1}).

At 1–30 min, a strong peak at 3605 cm^{-1} decreased significantly and the absorption band at 3600–3565 cm^{-1} increased. The other OH stretching bands still showed no changes. The peaks at 1604, 1582, 1290, and 1253 cm^{-1} exhibited significantly increased intensity, and the peak at 1506 cm^{-1} also became more intense. The peak at 1604 cm^{-1} became stronger than that at 1620 cm^{-1} after ∼8 min under UV irradiation. A slightly decreasing band at 1000–930 cm^{-1} was also observed in the spectrum of 30 min.

After 5 h of UV irradiation, the absorption bands at 3727, 3605, and 1000–900 cm^{-1} decreased, whereas those at 3565, 1582, 1506, 1290, 1253, and 1060–1003 cm^{-1} increased. The peak at 1582 cm^{-1} became more intense than the peak at 1604 cm^{-1}. The intensity of the peak at 1620 cm^{-1} remained unchanged.

Table 1 also lists the assignment of absorption bands on TiO_2 catalyst after UV was turned on. After UV irradiation, several new absorption bands appearing at 1604, 1582, and 1253 cm^{-1} were assigned to bidentate nitrate [6,8,9,20], and the peak at 1290 cm^{-1} was assigned to monodentate nitrate [6,8,9,20]. The absorption band at 1060–1003 cm^{-1} was assigned to nitrate, possibly in the bidentate state [10,11]. The absorption band at 1698 cm^{-1} after UV irradiation might be caused by residual contaminants on the TiO_2 surface activated by UV light.

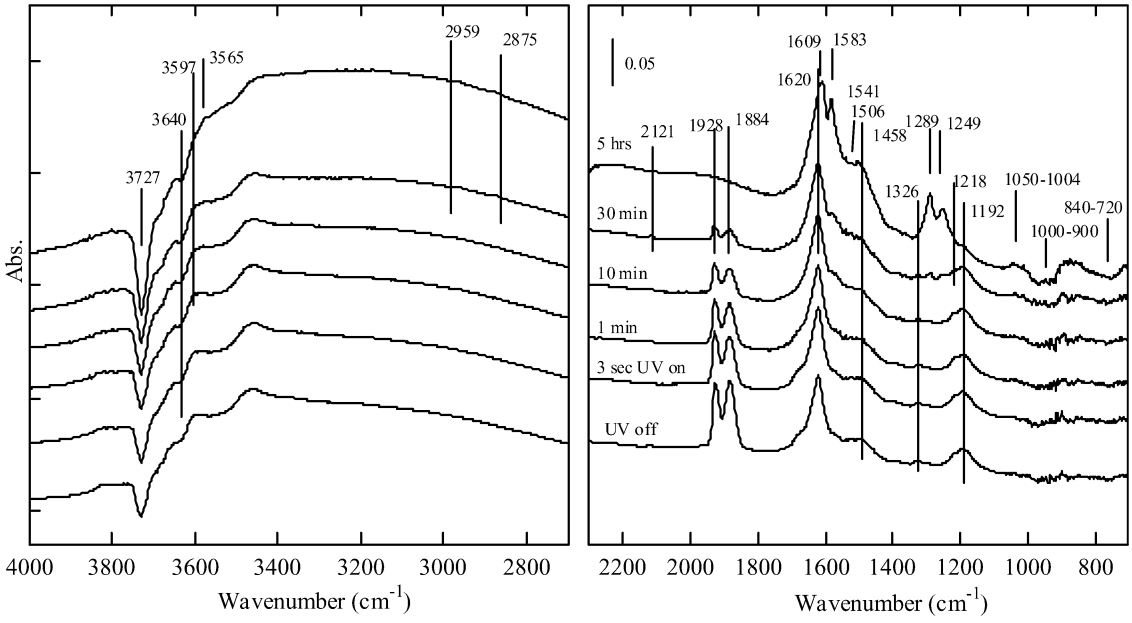

Fig. 7. IR spectra of photocatalytic reaction of NO on Cu/TiO_2 under UV irradiation.

3.3. Photocatalytic NO reaction on Cu/TiO_2

Fig. 7 shows the spectra of NO adsorbed on the Cu/TiO_2 in time sequences within 5 h under UV irradiation. The spectrum of "UV off" (i.e., before UV was turned on) was similar to the spectra of NO adsorbed on TiO_2 (Fig. 5), except for the appearance of sharp, strong absorption bands at 1928 and 1884 cm^{-1} and weak absorption bands at 2121, 1326, and 1218 cm^{-1}. Careful inspection of the band at 1928 cm^{-1} revealed that it was overlapped by a shoulder at 1919 cm^{-1}. After UV was turned on, in the high-frequency region, a peak at 3565 cm^{-1} increased in intensity, whereas a peak at 3640 cm^{-1} decreased in intensity after 10 min. In the low-frequency region, the peaks at 1928 and 1884 cm^{-1} decreased significantly and the band at 1580–1558 cm^{-1} increased gradually over 10 min.

Over the subsequent 30 min, the peaks at 3727 and 3597 cm^{-1} decreased slightly, and two very weak new bands at 2959 and 2875 cm^{-1} were detected. In the range of 650–2300 cm^{-1}, absorption bands at 1928, 1884, 1000–900, and 767 cm^{-1} decreased gradually, and new bands at 1583, 1541–1506, 1458, 1289, and 1249 cm^{-1} developed progressively. In contrast, the intensity of absorption bands at 1218 and 1192 cm^{-1} remained unchanged. After 5 h of UV irradiation, the peaks at 1928, 1884, and 1192 cm^{-1} diminished completely; those at 3727, 3597, 1000–900, and 840–720 cm^{-1} decreased; and those at 1609, 1583, 1541–1506, 1289, 1249, and 1050–1004 cm^{-1} evolved. The peak at 1609 cm^{-1} was more intense than the peaks at 1620 and 1583 cm^{-1}. A peak at 1326 cm^{-1} was possibly overlapped by the peaks at 1289 cm^{-1}. The band at 3565 cm^{-1} was overlapped by a very broad band from 3900 cm^{-1} to below than 2700 cm^{-1}.

Table 2 summarizes the assignment of all absorption bands on Cu/TiO_2 except those given in Table 1. Hadjiivanov [21] proposed that adsorption of NO on Cu^{2+} would form nitrosyls and produce different absorption bands in the IR spectra, ranging from 1964 to 1845 cm^{-1}. Davydov [19] and Lokhov and Davydov [22] also proposed that with Cu^{2+} supported on zeolites or metal oxides, such as Al_2O_3, three absorption bands at around 1950, 1920, and 1885 cm^{-1} may be detected by IR spectrometry. In particular, the peaks at 1920, 1900, and 1875 cm^{-1} were assigned to NO adsorbed on weakly associated Cu^{2+} (Cu–O–Al), isolated Cu^{2+}, and strongly associated Cu^{2+} (Cu–O–Cu, or CuO-like structure), respectively, on Cu/Al_2O_3. Accordingly, a peak at 1928 cm^{-1}, a shoulder at 1919 cm^{-1}, and a peak at 1884 cm^{-1} can be roughly assigned to NO adsorbed on weak associated Cu^{2+}, isolated Cu^{2+}, and strongly associated Cu^{2+}, respectively.

Table 2
Assignments of the FT-IR bands observed upon adsorption of NO on 2 wt% Cu/TiO_2 followed by UV irradiation

Wavenumbers (cm^{-1})	Assignment	References
1218	Nitrite adsorbed on Cu^{2+}, possibly in the bidentate state, $\nu(NO_2)$	[21,24]
1326	Adsorbed nitro compounds, $\nu(-NO_2)$	[21,23]
1884	NO adsorbed on strong associated Cu^{2+} (Cu–O–Cu, or CuO-like structure), ν(NO)	[19,21,22]
1919 shoulder	NO adsorbed on isolated Cu^{2+}, ν(NO)	[19,21,22]
1928	NO adsorbed on weak associated Cu^{2+}, ν(NO)	[19,21,22]
2121	NO_2^+, NO^+, $NO^{\delta+}$ on Cu^{2+}, $\nu(NO_2)$	[21,23,25]
2875	ν_s(CH)	[26–28]
2959	ν_{as}(CH)	[26–28]

The absorption bands at 1400–1300 cm^{-1} were assigned to nitro compounds ($-NO_2$) adsorbed on various metal oxides, including Cu^{2+} [21,23]. Therefore, the peak of 1326 cm^{-1} was assigned to nitro compounds. An absorption peak at 1218 cm^{-1} was assigned to nitrite adsorbed on Cu^{2+} [21,24], possibly in the bidentate state (similar to the peak at 1192 cm^{-1} on TiO_2 in Table 1). A peak at 2121 cm^{-1} was still uncertain; some

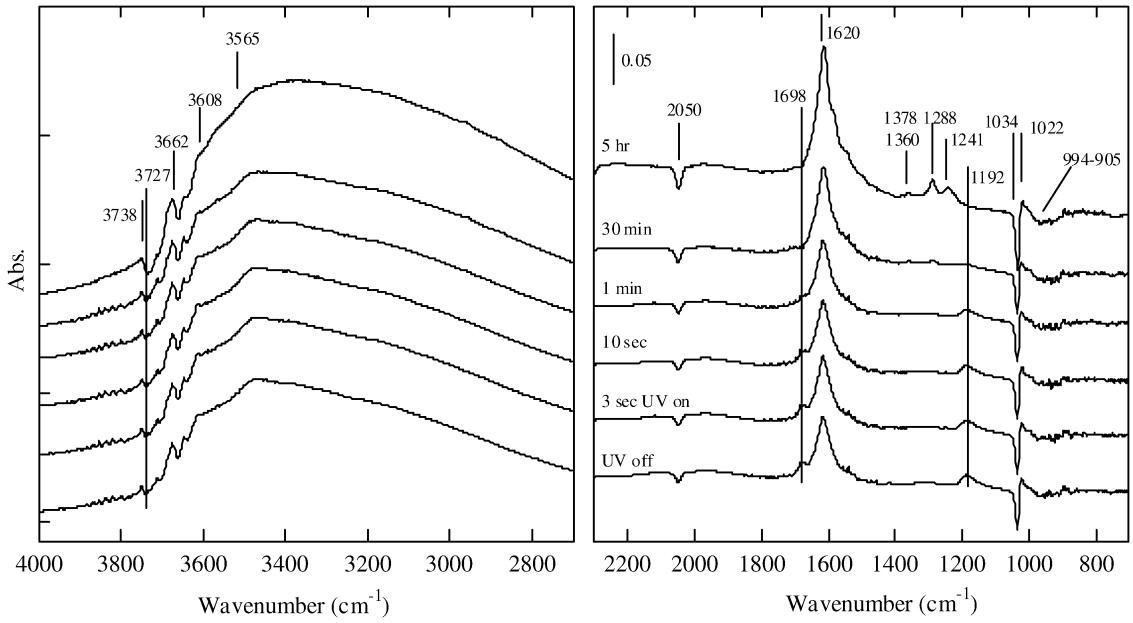

Fig. 8. IR spectra of photocatalytic reaction of NO on V/TiO_2 under UV irradiation.

researchers suggested assigning it to $NO_2^{\delta+}$, NO^+, or NO_2^+ adsorbed on Cu^{2+} [21,23,25]. The absorption band at 1580–1558 cm^{-1}, which increased within the first minute under UV irradiation, was assigned to bidentate nitrate adsorbed on the TiO_2 surface [6]. The bands at 2959 and 2875 cm^{-1} were assigned to ν_{as}(CH) and ν_s(CH) modes, respectively [26–28]. The appearance of CH bonds may be due to the photocatalytic reduction of trace amounts of CO_2 in the atmosphere [29].

3.4. Photocatalytic NO reaction on V/TiO_2 and Cr/TiO_2

Fig. 8 shows the spectra of NO adsorbed on 1.9 wt% V/TiO_2 over 5 h under UV irradiation. Before UV was turned on, the spectra were different than those of TiO_2 and Cu/TiO_2 catalysts in the OH-stretching region (4000–3000 cm^{-1}). Only small decreases at 3738 and 3727 cm^{-1} and a weak absorption band at 3608 cm^{-1} were observed on V/TiO_2. The peaks at 3566 cm^{-1} and a broad band at below 3550 cm^{-1} exhibited the same behavior as TiO_2 and Cu/TiO_2. The spectra in the region of 2300–650 cm^{-1} were mostly similar to those of TiO_2 and Cu/TiO_2, but additional absorption bands at 1698, 1022, and 1000–900 cm^{-1} (negative) and two sharp negative bands at 2050 and 1034 cm^{-1} were observed.

Virtually no changes in the spectra were observed during 30 min of UV irradiation, particularly in the OH-stretching region. New absorption bands at 1378, 1360, 1288, and 1241 cm^{-1} appeared in the 2300–650 cm^{-1} region, but these were of very weak intensity. The surface-contaminated peak at 1698 cm^{-1} exhibited a slight progressive decrease. Finally, after 5 h of UV irradiation, a slightly more intense peak at 3566 cm^{-1} occurred, possibly caused by extended bands of delocalized protons (at 3900–2500 cm^{-1}). In the 2300–650 cm^{-1} region, small decreases at 2050, 1034, and 1192 cm^{-1} and increasing bands at 1378, 1360, 1288, and 1241 cm^{-1} were observed, as were more negative bands at 1000–900 cm^{-1} characteristic of surface peroxo species.

Table 3
Assignments of the FTIR bands observed upon adsorption of NO on 1.9 wt% V/TiO_2 and 0.65 wt% Cr/TiO_2 followed by UV irradiation

Wavenumbers (cm^{-1})	Assignment	References
1017	Coordinatively unsaturated Cr=O	[33,34]
1034	Coordinatively unsaturated V=O	[7,31,32]
1381–1378, 1361–1360	Adsorbed nitro compounds, ν(–NO_2)	[21]
1923	Nitrosyl adsorbed on Cr ions having the oxidation state higher than +3, ν(–NO)	[21]
2020	Coordinatively unsaturated Cr=O, first overtone	[33,34]
2050	Coordinatively unsaturated V=O, first overtone	[7,31,32]
2200–1800, broad	Nitrosyl $NO^{\delta+}$ on V, ν(–NO)	[31]
3641	OH groups adsorbed on Cr atoms	[33]
3662	Surface OH groups adsorbed on V^{5+} cations	[30]

Table 3 summarizes the assignments of absorption bands of V/TiO_2 and Cr/TiO_2 (except for those given in Table 1). An absorption band at 3662 cm^{-1} was assigned to hydroxyl groups adsorbed on V^{5+}, a more highly electropositive surface metal cation than Ti^{4+} [30]. The sharp negative band at 1034 cm^{-1} was attributed to the disappearance of V=O, and another decrease at 2050 cm^{-1} was its first overtone [7,31,32]. The results of absorption bands at 2200–1800 cm^{-1} were consistent with the findings of Ramis et al. [31] and were assigned to surface nitrosyl species in the form of $NO^{\delta+}$. The peak at 1698 cm^{-1} might be caused by surface contaminants. The peaks at 1378 and 1360 cm^{-1} were assigned to nitro compounds [21].

Fig. 9 shows the spectra of NO adsorbed on 0.65 wt% Cr/TiO_2 catalyst over time under UV irradiation. Almost no changes in spectra were observed during the first minute, simi-

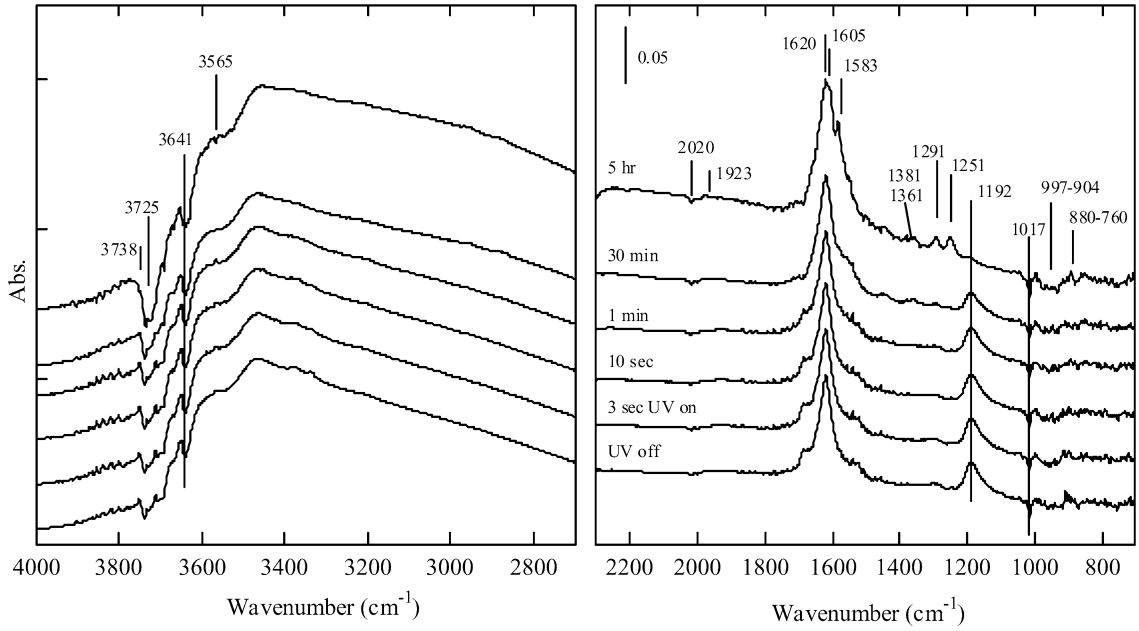

Fig. 9. IR spectra of photocatalytic reaction of NO on Cr/TiO_2 under UV irradiation.

lar to V/TiO_2. Only a slight decrease in the peak at 1192 cm^{-1} was detected. After UV irradiation for 30 min, the peak at 3565 cm^{-1} almost vanished, and new bands at 1381 and 1360 cm^{-1} appeared progressively. The peak at 1192 cm^{-1} decreased slightly. After 5 h of UV irradiation, the bands at 3738, 3725, and 3590–3565 cm^{-1} decreased further. In the 2300–650 cm^{-1} region, new absorption bands at 1605, 1583–1540, 1291 and 1251 cm^{-1} developed. The signal peak at 1192 cm^{-1} diminished but did not vanished completely. Moreover, decreases at the surface peroxo region (1000–900 cm^{-1}) were also observed. Note that the intensity of the peak at 1620 cm^{-1} did not change under UV irradiation.

The distinctive absorption bands of Cr/TiO_2 are also listed in Table 3. Before UV was turned on, the spectrum (UV off) was similar to that of V/TiO_2. In the 2300–650 cm^{-1}, region, a sharp decrease at 1017 cm^{-1} was attributed to the disappearance of Cr=O; a peak at 2020 cm^{-1} was its first overtone [33,34]. The weak negative band at 3641 cm^{-1} was assigned to OH groups adsorbed on Cr atoms [33]. Considering the π back-donation effect, a signal peaking at 1923 cm^{-1} was assigned to nitrosyl adsorbed on chromium ions ($<$2200 cm^{-1} for NO^+ free ion).

4. Discussion

4.1. NO adsorption on TiO_2

After thermal pretreatment in air, hydrocarbon contaminants on TiO_2 were mostly removed (1800–1200 cm^{-1}) except for the readsorbed H_2O and splitting OH groups. Zhang et al. [2] reported that H-bonded OH groups become free OH groups on high-temperature treatment. A large amount of H-bonded OH groups originally existed on the surface of sol–gel derived TiO_2, and thermal treatment made these OH groups dissociated. Thus the pretreated TiO_2 surface was clean, and only OH groups and very few H_2O existed under our experimental conditions.

Surface OH groups are known to play an important role when charged ions such as ammonium, alkoxide, or nitrate ions are adsorbed on TiO_2. Investigators have found that surface OH groups can act as Brönsted acid sites to donate protons when NH_3 is adsorbed on TiO_2, resulting in the consumption of OH groups and the formation of NH_4^+ ions [35,36]. Hadjiivanov [21] reported that adsorption of negatively charged ions on metal oxides, causes replacement of another negative fragment, such as the OH group. Similarly, Kantcheva [20] reported that the formation of nitrite or nitrate adsorbed on TiO_2 caused the consumption of OH groups, resulting in NOH.

The adsorption of NO on TiO_2 resulted in the formation of NOH, bidentate and monodentate nitrates, bidentate nitrite, TiOO– and other surface peroxides (750–680 cm^{-1}), as shown in Fig. 5. Surface free OH groups and surface peroxo species were consumed and transformed to another peroxo species in the structures of TiOO–. Hydroperoxo, TiOOH, was generated during NO adsorption, causing absorption bands at 870–770 cm^{-1} [14,17]. Protons in TiOOH may be from NOH species formed by the interaction of NO and free OH groups.

Lattice oxygen atoms also may be involved in the NO adsorption process. Our experimental results on thermal stability indicated that some surface peroxo species were removed and not completely restored after thermal pretreatment of TiO_2 under He flow. It is well known that metal oxide surfaces exhibit the defect of unsaturated coordination [19]. Accordingly, the surface of pretreated TiO_2 had large amounts of active oxygen atoms and oxygen vacancies, which were involved in the formation of bidentate nitrite when NO was adsorbed on TiO_2.

A proposed possible mechanism of NO adsorption is shown in Scheme 1. NO preferentially attacks surface free OH groups and is oxidized to monodentate nitrite by surface active oxygen (i.e., coordination unsaturated oxygen). Then the oxygen vacancy and surface peroxo species induce the transformation

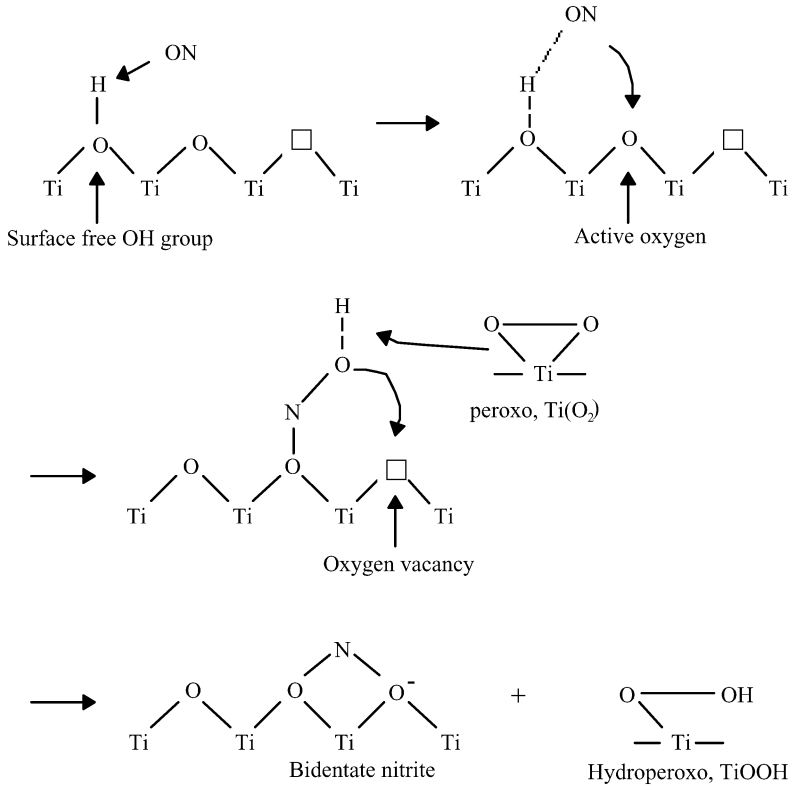

Scheme 1. A possible mechanism of NO adsorption on TiO_2.

of monodentate nitrite to bidentate nitrite, and a hydroperoxo is generated.

Fig. 5 also shows some weak peaks at 1508–1576 cm^{-1} indicating formation of monodentate and bidentate nitrates, and these nitrates were coupled with OH groups (1668–1620 cm^{-1}) for extended periods (>20–30 min). These nitrates may be formed by further oxidation of monodentate and bidentate nitrites by surface peroxo species or active oxygen atoms. However, monodentate nitrite was not detected, because its lifetime was short with the NOH bond, which was quickly transformed to bidentate nitrite, monodentate, or bidentate nitrates.

4.2. Photocatalytic NO reaction on TiO_2

As shown in Fig. 6, UV irradiation for 3–10 s resulted in a rapid decrease in bidentate nitrite (1192 cm^{-1}) and an increase in monodentate and bidentate nitrates. The 1- to 30-min UV irradiation resulted in the absence of bidentate nitrite and a decrease in surface peroxo species in the structure of $Ti(O_2)$ (at 1000–900 cm^{-1}) and H-bonded OH groups peaked at 3605 cm^{-1}. Finally the 5 h of UV irradiation further increased nitrates and decreased $Ti(O_2)$ and free OH groups (at 3727 cm^{-1}). In addition, the peak at 3565 cm^{-1} became more intense after 5 h of UV irradiation, indicating an increasing number of OH groups coupled by nitrates. It is noteworthy that the increase in nitrates and decrease in surface peroxo species occurred simultaneously.

In general, electron–hole pairs are photogenerated in a semiconductor such as TiO_2 under UV irradiation, after which a photocatalytic reaction can be initiated. Nakamura et al. [14,17] suggested that surface superoxo species, TiOO•, were photogenerated under UV irradiation. However, because the superoxo species are extremely active and have short lifetimes, they cannot be detected due to the limitation of IR measurement. An intermediate, superoxo, photogenerated from $Ti(O_2)$ is suggested to dominate photocatalytic NO oxidation. The photocatalytic oxidation of nitrites to nitrates is attributed mostly to photogenerated surface superoxo species.

The formation of oxygen vacancies plays an important role in photocatalysis. Fujishima et al. [37] reported that under UV irradiation, surface oxygen atoms are oxidized to oxygen molecules by photogenerated holes, leaving oxygen vacancies. H_2O molecules can then be adsorbed on oxygen vacancies and split into OH groups. Oxygen vacancies or other active species, such as oxygen molecules, may be photogenerated during UV irradiation, but H_2O molecules were scarce under our experimental conditions. Although the oxidation of monodentate or bidentate nitrite by oxygen molecules may be possible, its rate would be much slower than that by superoxo.

A proposed photocatalytic mechanism of NO oxidation is shown in Scheme 2. Electron–hole pairs are photogenerated under UV irradiation; then the holes are trapped by surface peroxo species, which in turn are transformed to superoxo species. Adsorbed bidentate nitrite is oxidized to either monodentate or bidentate nitrate by reaction with superoxo species. If the superoxo species do not contact with nitrites, then they are further photo-oxidized to oxygen molecules, leaving oxygen vacancies.

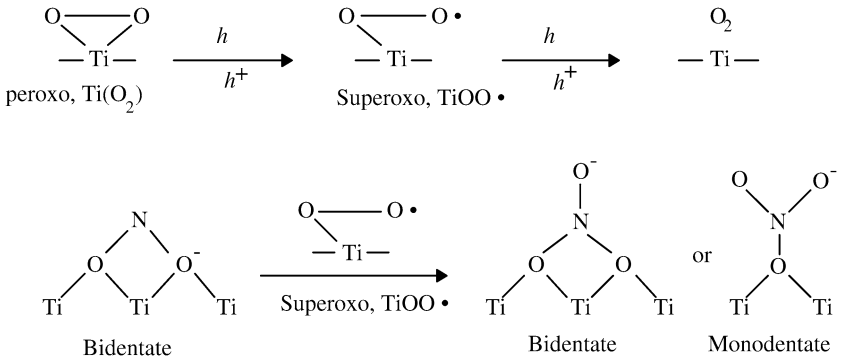

Scheme 2. A possible mechanism of photocatalytic NO oxidation on TiO_2.

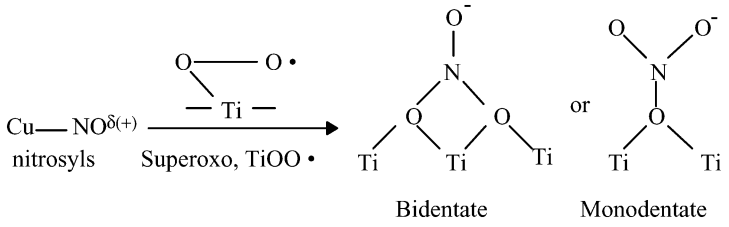

Scheme 4. A possible mechanism of photocatalytic NO oxidation on 2 wt% Cu/TiO_2.

4.3. Photocatalytic NO reaction on 2 wt% Cu/TiO_2

Before UV irradiation, bidentate nitrite and monodentate nitrate adsorbed on Cu/TiO_2 were observed as shown in Fig. 7, similar to the spectra of NO adsorption on TiO_2. The same mechanism outlined in Scheme 1 was also applied to Cu/TiO_2. However, significant differences were found; bidentate nitrite (at 1218 cm^{-1}) and nitrosyls (at 1928 and 1884 cm^{-1}) adsorbed on Cu^{2+} and adsorbed nitro compounds (at 1326 cm^{-1}) were also detected. NO molecules were also adsorbed on Cu^{2+} ions, forming nitrosyls, as shown in Scheme 3. The vibration frequencies of nitrosyls were higher than those of NO molecules (1876 cm^{-1}) but lower than those of NO^+ free ions ($\sim$2200 cm^{-1}), suggesting that the electrons of NO were drawn to Cu^{2+}. But the electrons were not completely transferred to Cu^{2+}, because of the π back-donation effect; thus the Cu^{2+} ions were not reduced to Cu^+. Adsorbed nitrosyls may be further oxidized to nitro compounds by active oxygen or peroxo species.

As shown in Fig. 7, 30 min of UV irradiation caused a decrease in all nitrosyl bands and surface peroxo species and an increase in monodentate and bidentate nitrates (at 1583, 1550–1500, and 1458 cm^{-1}). The absorption bands characteristic of bidentate nitrites and nitro compounds showed no changes. Thus nitrate formation was attributed to the oxidation of nitrosyls. The oxidation reaction was induced by photogenerated superoxo species, TiOO•, similar to those on TiO_2.

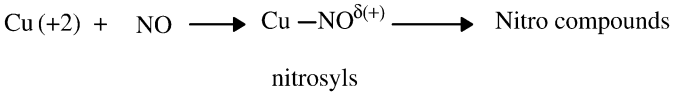

Scheme 3. Formation of nitrosyls adsorbed on Cu^{2+} ions.

The spectrum of long-term (5 h) UV irradiation on Cu/TiO_2 was very similar to that on TiO_2. The adsorbed nitrosyls vanished, and the significant signals characteristic of monodentate and bidentate nitrates were fully developed. The oxidation from nitrites to nitrates can also be carried out under UV irradiation on the Cu/TiO_2 catalysts; however such an oxidation reaction was not observed in the first 30 min. This suggests that the superoxo species preferentially oxidize adsorbed nitrosyls or, in other words, that the oxidation of nitrites to nitrates is deferred by adsorbed nitrosyls. Because the nitrosyls are partially positively charged compounds and the bidentate nitrites are negatively charged compounds, it is reasonable to expect that the extremely negatively charged superoxo species will preferentially attack the adsorbed nitrosyls. Scheme 4 briefly shows a possible mechanism of nitrosyl oxidation on 2 wt% Cu/TiO_2 catalyst.

Although isolated weakly associated and strongly associated Cu^{2+} existed on the catalyst surface, there was no evidence indicating which species caused the formation of bidentate nitrite adsorbed on Cu^{2+}. This may be caused by Cu^{2+} ions in different structures (at 1928, 1919, and 1884 cm^{-1}) or by surface peroxo species, such as $Ti(O_2)$. Distinguishing whether or not nitro compounds were decreased under UV irradiation was difficult, because the absorption band of these compounds at 1326 cm^{-1} was overlapped by the peak at 1289 cm^{-1}.

4.4. Photocatalytic NO reactions on 1.9 wt% V/TiO_2 and 0.65 wt% Cr/TiO_2

Photocatalytic NO oxidation on V/TiO_2 and Cr/TiO_2 exhibited similar behavior. The adsorption of NO on V/TiO_2 and Cr/TiO_2 caused sharp decreases in the bands characteristic of coordination-unsaturated V=O and Cr=O bonds, respectively.

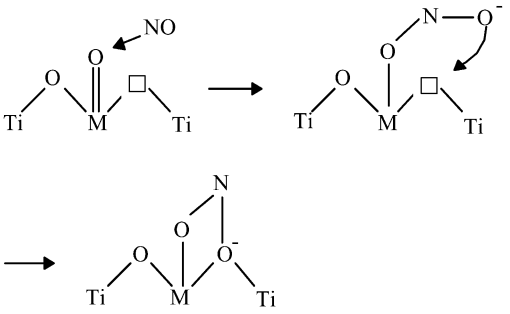

Scheme 5. A possible mechanism of NO adsorption on 1.9 wt% V/TiO_2 or 0.65 wt% Cr/TiO_2 (M = V or Cr).

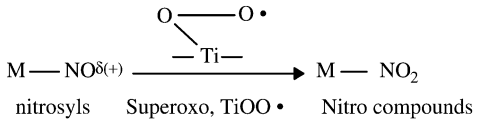

Scheme 6. A possible mechanism of photocatalytic oxidation from nitrosyls to nitro compounds.

The intensity of absorption bands characteristic of bidentate nitrites peaking at around 1192 cm^{-1} was higher than that of TiO_2, especially for Cr/TiO_2. Moreover, on TiO_2, NO was also trapped on V=O or Cr=O and was then oxidized to nitrites. A proposed mechanism for the adsorption of NO on V/TiO_2 or Cr/TiO_2 is shown in Scheme 5. NO is adsorbed on V=O or Cr=O, then transformed to bidentate nitrite via oxygen vacancy.

The ability of photocatalytic NO oxidation on these two catalysts was very poor under UV irradiation. In the first minute, only a decrease in the hydroxyl groups adsorbed on Cr was observed; the nitrosyls and bidentate nitrites showed no changes. After 30 min of UV irradiation, only a slight decrease in bidentate nitrites and a slight increase in nitro compounds and nitrates were detected. These changes were very small compared with those on TiO_2 and Cu/TiO_2 catalysts during 30 min of UV irradiation. After 5 h of UV irradiation, monodentate and bidentate nitrates were observed, and trace amounts of bidentate nitrites remained. Careful inspection of the absorption bands characteristic of peroxo species and nitro compounds revealed that these decreased continuously under UV irradiation, but at much slower rates of change than those for TiO_2 and Cu/TiO_2 catalysts. The adsorbed nitrosyls showed very little decrease in the first 30 min, but this region (2200–1800 cm^{-1}) was perturbed by the baseline shifts in the 5-h UV irradiation spectrum (Figs. 8 and 9) and so was unclear in the long term.

As shown in Scheme 6, the formation of nitro compounds is caused by oxidation of nitrosyls. The superoxo species preferentially oxidize compounds adsorbed on doping V or Cr ions, similar to photocatalytic NO oxidation on Cu/TiO_2 but in only small amounts. The weak decreases in the bands characteristic of peroxo species, $Ti(O_2)$, under UV irradiation indicated that only a portion of the photogenerated holes converted peroxo species to superoxo species. Hole scavengers, such as defect sites, may exist on the surface of V/TiO_2 and Cr/TiO_2, draining photogenerated holes.

5. Conclusion

All of the catalysts studied (TiO_2, 2 wt% Cu/TiO_2, 1.9 wt% V/TiO_2, and 0.65 wt% Cr/TiO_2) exhibited the capability for photocatalytic NO oxidation. Various intermediate species were observed from this in situ FTIR study. The adsorption and photocatalytic reaction of NO on catalysts involved various types of active intermediates formed by surface active species and photogenerated holes. Nitric oxide could be adsorbed in the form of bidentate nitrites by reacting with surface free OH groups. Nitrates were produced with consumption of peroxo species. During UV irradiation, surface peroxo species were oxidized to superoxo species by photogenerated holes, and then bidentate nitrites were oxidized to nitrates by superoxo species.

Pure TiO_2 demonstrated the most powerful activity for photocatalytic NO oxidation. Under UV irradiation, most adsorbed nitrites were transformed to nitrates within seconds, and no other species were found. For Cu/TiO_2, adsorption of NO caused not only the formation of nitrites adsorbed on TiO_2 and Cu^{2+}, but also the formation of nitrosyls adsorbed on Cu^{2+}. Under UV irradiation, photogenerated superoxo species preferentially oxidized nitrosyls, thereby deferring the oxidation of nitrites to nitrates. For V/TiO_2 and Cr/TiO_2, the photocatalytic oxidation of nitrites was strongly inhibited because the superoxo species preferentially oxidize nitrosyls or hydroxyl groups adsorbed on V or Cr ions. Hole scavengers may exist in these two catalysts, resulting in less peroxo species oxidized to superoxo species. Consequently, the oxidation rate of nitrites to nitrates was significantly decreased on V/TiO_2 and Cr/TiO_2.

Acknowledgments

Financial support was provided by the National Science Council, Taiwan (grant NSC93-EPA-Z-002-006) and the Ministry of Economic Affairs, Taiwan (grant 93-EC-17-A-09-S1-019). The authors thank the Nano Research Center of National Taiwan University for providing the IR instrument.

References

[1] J. Zhang, T. Ayusawa, M. Minagawa, K. Kinugawa, H. Yamashita, M. Matsuoka, M. Anpo, J. Catal. 198 (2001) 1.
[2] T.H. Lim, S.M. Jeong, S.D. Kim, J. Gyenis, J. Photochem. Photobiol. A Chem. 134 (2000) 209.
[3] B.J. Lee, M.C. Kuo, S.H. Chien, Res. Chem. Intermed. 29 (2003) 817.
[4] I.-H. Tseng, W.-C. Chang, J.C.S. Wu, Appl. Catal. B 37 (2002) 37.
[5] Jeffrey C.-S. Wu, C.-H. Chen, J. Photochem. Photobiol. A: Chem. 163 (2004) 509.
[6] K. Hadjiivanov, V. Bushev, M. Kantcheva, D. Klissurski, Langmuir 10 (1994) 464.
[7] C.-H. Lin, H. Bai, Ind. & Eng. Chem. Research 43 (2004) 5983.
[8] G. Ramis, G. Busca, V. Lorenzelli, P. Rorzatti, Appl. Catal. 64 (1990) 243.
[9] M.M. Kantcheva, V.Ph. Bushev, K.I. Hadjiivanov, J. Chem. Soc., Faraday Trans. 88 (1992) 3087.
[10] I. Nakamura, S. Sugihara, K. Takeuchi, Chem. Lett. 11 (2000) 1276.
[11] D.V. Pozdnyakov, V.N. Fillmonov, Kinet. Catal. 14 (1973) 655.
[12] K. Hadjiivanov, H. Knozinger, Phys. Chem. Chem. Phys. 2 (2000) 2803.
[13] K. Hadjiivanov, P. Conception, H. Knozinger, Top. Catal. 11/12 (2003) 123.
[14] R. Nakamura, A. Imanishi, K. Murakoshi, Y. Nakato, J. Am. Chem. Soc. 125 (2003) 7443.

[15] T. Ohno, Y. Masaki, S. Hirayama, M. Matsumura, J. Catal. 204 (2001) 163.
[16] G. Munuera, A.R. Gonzalez-Elipe, A. Fernandez, P. Malet, J.P. Espinos, J. Chem. Soc., Faraday Trans. I 85 (1989) 1279.
[17] R. Nakamura, Y. Nakata, J. Am. Chem. Soc. 126 (2004) 1290.
[18] R.D. Jones, D.A. Summerville, F. Basolo, Chem. Rev. 79 (1979) 139.
[19] A.A. Davydov, in: C.H. Rochester (Ed.), Infrared Spectroscopy of Adsorbed Species on the Surface of Transition Metal Oxides, John Wiley and Sons, Chichester, New York, 1990, pp. 6–7, 25, 33–35, 64–69.
[20] M. Kantcheva, J. Catal. 204 (2001) 479.
[21] K.I. Hadjiivanov, Catal. Rev. 42 (2000) 71.
[22] Y. Lokhov, A. Davydov, Kinet. Catal. 21 (1980) 943.
[23] J. Valyon, W.K. Hall, J. Phys. Chem. 97 (1993) 1204.
[24] A. Davydov, A. Budneva, React. Kinet. Catal. L. 25 (1984) 121.
[25] A.W. Aylor, S.C. Larsen, J.A. Reimer, A.T. Bell, J. Catal. 157 (1995) 592.
[26] J.M. Coronado, S. Kataoka, I.T. Tejedor, M.A. Anderson, J. Catal. 219 (2003) 219.
[27] W.C. Wu, C.C. Chuang, J.L. Lin, J. Phys. Chem. B 104 (2000) 8719.
[28] R. Nakamura, J. Phys. Chem. B 106 (2002) 5893.
[29] I.H. Tseng, Jeffrey C.S. Wu, H.Y. Chou, J. Catal. 221 (2004) 432.
[30] N.Y. Topsoe, J. Catal. 128 (1991) 499.
[31] G. Ramis, G. Busca, F. Bregani, P. Forzatti, Appl. Catal. 64 (1990) 259.
[32] C. H Lin, H. Bai, Appl. Catal. B 42 (2003) 279.
[33] M.S. Marth, A. Wokaun, H.E.C. Hyde, A. Baiker, J. Catal. 133 (1992) 415.
[34] U. Scharf, H. Schneider, A. Baiker, A. Wokaun, J. Catal. 145 (1994) 464.
[35] G. Busca, H. Saussey, O. Saur, J.C. Lavalley, V. Lorenzelli, Appl. Catal. 14 (1985) 245.
[36] J.M. Watson, U.S. Ozkan, J. Mol. Catal. A 192 (2003) 79.
[37] A. Fujishima, T.N. Rao, D.A. Tryk, J. Photochem. Photobiol. C Photochem. Rev. 1 (2000) 1.